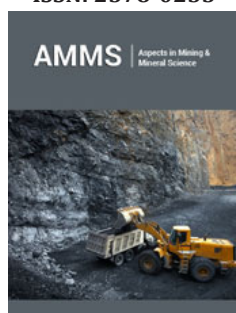


# Comparison of Bubble Diameters Measured from Photographs with those Estimated by Drift Flux and Predicted by CFD in An Air-Water Flotation System

ISSN: 2578-0255



José Guadalupe González V<sup>1</sup>, Ramiro Escudero García<sup>1\*</sup>, Hugo Arcos Gutiérrez<sup>2</sup>, Martín Reyes P<sup>3</sup> and Noemí Ortiz L<sup>1</sup>

<sup>1</sup>Metallurgy and Materials Research Institute, Michoacán University of San Nicolás de Hidalgo, Mexico

<sup>2</sup>Conacyt-Ciateq, Mexico

<sup>3</sup>Academic Area of Earth and Materials Sciences, Autonomous University of the State of Hidalgo, Mexico

**\*Corresponding author:** Ramiro Escudero García, Metallurgy and Materials Research Institute, Michoacán University of San Nicolás de Hidalgo, Santiago Tapia 403. Zip Code 58000, Morelia, Michoacán, Mexico

**Submission:**  February 28, 2025

**Published:**  March 18, 2025

Volume 13 - Issue 2

**How to cite this article:** José Guadalupe González V, Ramiro Escudero García\*, Hugo Arcos Gutiérrez, Martín Reyes P and Noemí Ortiz L. Comparison of Bubble Diameters Measured from Photographs with those Estimated by Drift Flux and Predicted by CFD in An Air-Water Flotation System. *Aspects Min Miner Sci.* 13(2). AMMS. 000807. 2025. DOI: [10.31031/AMMS.2025.13.000807](https://doi.org/10.31031/AMMS.2025.13.000807)

**Copyright@** Ramiro Escudero García, This article is distributed under the terms of the Creative Commons Attribution 4.0 International License, which permits unrestricted use and redistribution provided that the original author and source are credited.

## Abstract

Column flotation is a technique used to recover particles or species of interest in air-water-particle or air-water systems. Air or gas is fed under pressure through dispersers or mechanical means to generate the dispersed phase in the continuous phase. Dispersion characteristics (bubble diameter, gas volume and bubble surface area) are a very important aspect that must be adjusted to each separation application and on which the capture and recovery efficiency of valuable species depends; unfortunately, the average bubble diameter cannot be measured directly in practice because flotation devices are not transparent; moreover, there is no control over the characteristics of the dispersions generated by most gas dispersers; in this last case, effective and reliable simulation of gas dispersers becomes important to control the characteristics of the dispersion that suits each specific application, whether mineral or non-mineral. In this work, the diameters of bubbles generated by a venturi-type disperser installed in a transparent laboratory flotation column were measured. These diameters measured from photographic evidence were compared with the bubble sizes estimated by solving the Drift Flux model and with the diameters predicted by the CFD simulation of the laboratory column used.

The comparison results shows that the measured, estimated and predicted bubble diameters reasonably converge within a difference range of less than 20%. The above allows us to establish the feasibility of controlling the characteristics of the dispersion of gases generated with the venturi, and to estimate with reasonable precision the characteristics of the dispersion generated in an air-water system, in addition to concluding that the design through CFD simulation of venturi-type dispersers under particular operating conditions of a flotation device is reliable.

**Keywords:** Bubble diameter; Drift flux; CFD; Column flotation; Bubble surface area flux

## Introduction

Flotation techniques originally designed to process mineral powders are now used in non-mineral systems, for example, to separate organic contaminants from water, heavy metals, paper deinking, separation of fats, oils and hydrocarbons, etc. In flotation, the interaction between continuous and dispersed phases occurs; the continuous phase is invariably water and the dispersed phases can be air, mineral particles, organic droplets, even species in solution

that contaminate water tables such as heavy metals constitute a continuous phase; in the latter case, the interaction occurs between the liquid-liquid-gas phases.

Research on flotation efficiency largely focuses on the effect of gas dispersion characteristics (bubble or droplet diameter, gas or droplet volume fraction, and bubble or droplet surface area); although their importance is recognized, there is no established way to control these dispersion characteristics for particular separation applications [1]. In a flotation column, the diameter of the bubbles ( $D_b$ ) depends on the type of gas disperser installed, the gas flow fed to the disperser, the surface tension of the continuous medium, the velocities of the phases in the column; in addition to knowing that this diameter varies with the height in the collection zone, due to the coalescence of bubbles and the expansion of the gas that forms them [2]. It is widely recognized that the characteristics of the dispersion are directly related to the hydrodynamics, mass transfer and efficiency of the dispersion equipment, however, in industrial processes there are no conditions that allow working in the laminar regime where clouds of bubbles of homogeneous diameter are generated [2-6], even in industrial practice, the average theoretical bubble diameter is not determined, so one cannot speak of control of the dispersion characteristics.

From the above, the importance of designing discontinuous phase dispersers with which it is possible to control the dispersion characteristics for specific separation applications is established. This research presents a modified venturi disperser, previously designed using Computational Fluid Dynamics (CFD) simulation. This technique is used to model and analyse the behaviour of a gas disperser in complex systems, such as flotation systems. CFD simulation allows to virtually recreate the interactions between fluid, gas bubbles and solid particles, providing a detailed analysis of operational variables such as fluid velocity, pressure and turbulence [7], and predicting dispersion characteristics under specific conditions of air and gas flows, pulp density, and viscosity of the continuous medium.

On the other hand, it is required to calculate the average bubble diameter that is sufficiently reliable or close to the actual diameter that is being generated through the venturi-type disperser installed in a flotation column, in order to then compare it with the one predicted through CFD. The drag or phase flow model, known as Drift Flux, is a series of equations that when solved iteratively results in an estimated average diameter based on knowing the air and water flows fed to the column, the viscosity and density values of the mineral pulp, and the volume of gas in the collection zone of the flotation device [8]. This research compares the bubble diameters calculated and estimated in three ways: using the Drift Flux model from the information collected from experiments in a laboratory flotation column, the one predicted by the CFD simulation of the column operation, and the one from the photographic evidence of the bubbles generated in the laboratory flotation column; the above simulating and using a modified venturi disperser for the air-water system.

## Theoretical Basis

Flotation is a selective phase separation operation in which physical and chemical phenomena take place. Separation is achieved by inducing contact between bubbles and hydrophobic particles or species. Bubbles are generated by feeding compressed air into a porous medium or bubble generator which distributes the bubbles in the collection zone of the column. The hydrophobic species captured by the bubbles continue their upward path in the column and exit the column at the top as a concentrate of valuable species, having previously passed through a foam zone or a concentrate washing zone [8,9]. The probability of contact between bubbles and hydrophobic species increases with the appropriate bubble size; that is, bubbles that, when capturing a certain species, have a diameter sufficient to ascend and exit the column, but this diameter is not so large that their residence time in the collection zone is relatively short and their ascent speed is so fast that there is no bubble-hydrophobic species contact; therefore, it is established with certainty that the  $D_b$  and the other characteristics of the dispersion define the efficiency of the recovery of valuable species.

### Gas holdup ( $\epsilon_g$ )

The gas holdup ( $\epsilon_g$ ) is the volume of air that accumulates in an area of the column, by the sum of the volumes of the gas bubbles [10], generally expressed as a percentage of volume. The appropriate  $\epsilon_g$  value is sufficient to capture and retain the largest amount of valuable mass;  $\epsilon_g$  is calculated by the difference in pressure drops in a certain portion of the column, and knowing the distance between the taps of this hydrostatic pressure, or by measuring the height of the liquid before and after injecting the gas [11], although the latter case refers to a stationary system which is not possible in industrial practice.

### Gas bubbles

Once a bubble overcomes mainly the inertial and viscous forces, it detaches from the bubble generator and rises due to the buoyancy force. The diameter of the bubbles will depend on the time it takes to overcome the forces that keep them attached to the disperser [12]; in addition to the above, due to the compressibility of the gas, the bubbles slightly increase their diameter as they rise and leave the flotation column.

### Bubble surface area flux ( $S_b$ )

1.1.1. Bubble surface area ( $S_b$ ): The bubble surface area is the sum of the surface areas of bubbles crossing a unit cross-sectional area of the column per unit time. Finch & Dobby [8] derive the following expression from mathematical analysis:

$$S_b = \frac{6J_g}{D_b} \quad (1)$$

Where  $S_b$  is the surface area of bubbles,  $D_b$  the average diameter of bubbles in cm, and  $J_g$  is the surface flow of air fed to the disperser (cm/s), calculated from the following equation:

$$J_g = \frac{Q_g}{A_c} \quad (2)$$

Where  $A_c$  is the cross-sectional area of the column ( $\text{cm}^2$ ). From equation (1) it follows that as  $D_b$  decreases,  $S_b$  increases and there is more surface area to capture and retain valuable hydrophobic species and increase flotation efficiency.

### Bubble diameter measurement ( $D_b$ )

The measurement of  $D_b$  is a problem due to the lack of reliable measurement techniques [13]. The main methods are: high-speed photography, electrical impedance tomography, capillary suction probes, optical tomography, optical endoscopic sensors, capacitance probes, and passive acoustic detection, among others [14]. When analysing bubble formation, size and behaviour, the most commonly used methods are imaging with a stroboscope, high-speed photography, or the use of X-rays.

### $D_b$ estimation by solving the drift flux model

The drag model, relative velocity between phases or Drift Flux, is a set of equations that estimates an average  $D_b$  in a flotation equipment after iteratively solving these equations [15]. The relative velocity ( $U_{sb}$ ) between the bubble phases and the liquid is defined by the following expression:

$$U_{sb} = \frac{J_g}{\varepsilon_g} + \frac{J_l}{1 - \varepsilon_g} \quad (3)$$

The relative velocity ( $U_{sb}$ ) is related to the terminal velocity ( $U_t$ ) of a bubble generated in a medium of infinite depth, with the following expression (for  $\varepsilon_g$  less than 30%):

$$U_{sb} = U_t (1 - \varepsilon_g)^{m-1} \quad (4)$$

where  $m$  depends on the Reynolds number of the bubble ( $Re_b$ ):

$$m = \left( 4.45 + 18 \frac{d_b}{d_c} \right) Re_b^{-0.1} \quad 1 < Re_b < 200 \quad (5)$$

$$m = 4.45 Re_b^{-0.1} \quad 200 < Re_b < 500 \quad (6)$$

The Reynolds number of the bubble is defined as:

$$Re_b = \frac{U_t \cdot \rho_{sl} \cdot d_b}{\mu_{sl}} \quad (7)$$

Combining equations (3) and (4) gives:

$$U_t = \frac{J_g}{\varepsilon_g (1 - \varepsilon_g)^{m-1}} + \frac{J_l}{(1 - \varepsilon_g)^{m-1}} \quad (8)$$

Some authors [16], adapt the equation that represents the relative velocity between phases and the  $D_b$  in a sedimentation system as follows:

$$U_{sb} = \frac{g \cdot d_b^2 \cdot (\rho_{sl} - \rho_b) (1 - \varepsilon_g)^{m-1}}{18 \mu_{sl} (1 + 0.15 Re_s^{0.687})} \quad (9)$$

The Reynolds number ( $Re_s$ ) of the bubble swarm is defined as:

$$Re_s = \frac{d_b \cdot U_{sb} \cdot \rho_{sl} (1 - \varepsilon_g)}{\mu_{sl}} \quad (10)$$

By solving for  $U_t$  from equation (3) and equating it with equation (8), we obtain:

$$U_t = \frac{\left( \frac{J_g}{\varepsilon_g} + \frac{J_l}{1 - \varepsilon_g} \right)}{(1 - \varepsilon_g)^{m-1}} \quad (11)$$

or

$$U_t = \frac{g \cdot d_b^2 \cdot (\rho_{sl} - \rho_b) (1 - \varepsilon_g)^{m-1}}{18 \mu_{sl} (1 + 0.15 Re_s^{0.687})} \quad (12)$$

To find the average  $D_b$ , it is necessary to solve the above equations in an iterative manner; in addition, it is essential to know some properties of the medium (the density of the liquid phase  $\rho_{sl}$  and of the gas phase  $\rho_b$ , the viscosity of the liquid phase  $\mu_{sl}$ ) as well as some variables of the system (surface velocity of gas  $J_g$  and of liquid  $J_l$ , as well as  $\varepsilon_g$ ). The algorithm used for the solution of the equations has already been described by some researchers [15].

### $D_b$ measurement by photographic techniques

Evidence of the size and shape of bubbles is obtained by means of photographic techniques. Given its simplicity, this technique is widely used [3-5,10,17-19]. Despite the mentioned advantage, the application of this method is restricted to transparent or semi-transparent systems and close to the wall of the equipment [12]. Although the results obtained with this technique are excellent, its reliability decreases if the system has many moving particles, if there is excessive turbulence or if the system presents curvature, for example, a cylindrical section [14]. Recently, devices have been designed that counteract these drawbacks and have given good results [19,20].

### $D_b$ prediction by CFD simulation

Atypical three-dimensional fluid flow models solve the continuity equation and the Navier-Stokes equations for incompressible Newtonian fluids which are based on the conservation of mass, and momentum at each point in the domain. The solution of these equations provides the pressure and velocity components at each point in the domain. At the high flow velocities involved in this process, such models must incorporate turbulent fluid flow. To fully describe the flow of a fluid, it is necessary to know the following properties of the system: Density ( $\rho$ ), Pressure ( $P$ ) and velocities in the three spatial directions of the problem ( $u, v, w$ ) corresponding to the axes ( $x, y, z$ ). Since the system consists of 6 unknowns, six equations are needed to find the solution to the three-dimensional flow. Together with the ideal gas law, the remaining five equations are the Navier-Stokes equations [3,4]. The equations formulated by Claude-Louis Navier in 1822 and independently derived by George Gabriel Stokes in 1845 correctly model Newtonian fluid flow; they consist of a set of nonlinear partial differential equations derived from the mass and momentum conservation equations. Due to the complexity of their solution, computerized routines are applied.

### Experimental Setup

Experiments were carried out in the air-water system, using a flotation column of 0.10m diameter and 2.60m height, made

of transparent acrylic material (Figure 1); this column has a square section at the top that allows photographing the bubbles generated by the venturi disperser at the base of the column. The cross-sectional area of the square section is equal to the area of the cylindrical section; this prevents distorting or destroying the bubbles by changing the geometry of the circular and flat sections. A venturi-type disperser was installed with inlet and outlet diameters of 0.0381m and 0.0127cm in the vena contract (diameter

ratio equal to 3). The water flow, previously conditioned in a mixing tank, was fed to the column by a centrifugal pump (Ql) and varied from 4 to 8L/min; compressed air (Qg) was fed to the disperser at flows of 4 to 10L/min. Both air and water flows were measured using sphere rotameters. A total of 35 combinations of Ql, and Qg flow rates were tested; the surface tension of the liquid was set at 55 dynes/cm by adding pine oil as a surfactant.

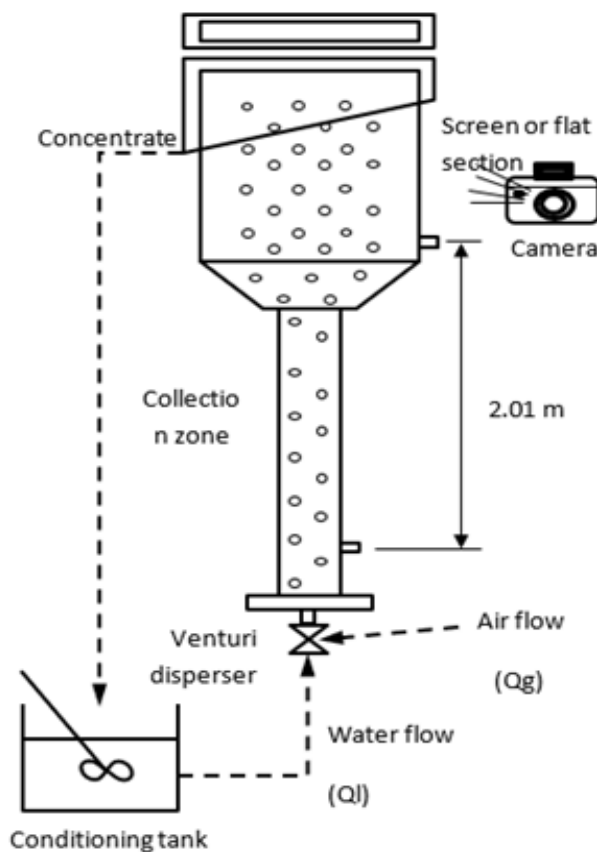


**Figure 1:** Experimental setup to obtain the values of Ql, Qg, and the pressure differentials ( $\Delta p$ ) to estimate  $D_b$  using Drift Flux, and photographs of the bubble swarm.

Using sensors, a data acquisition card, and a routine developed in LabView®, the hydrostatic pressures were measured at two points in the column (in the collection area), separated by 201cm, to calculate the gas volume ( $\epsilon_g$ ) and subsequently the  $D_b$  with the Drift Flux model. To capture photographs of the bubble swarm in each experiment, a digital camera was used with the capture parameters shown in Table 1. To measure the bubbles in the photographs, an image analyser included in the AutoCAD® software was used; at least 500 bubbles were measured in each photograph to subsequently establish the  $D_{b80}$ , which represents 80% of bubbles with a diameter less than a certain value. The calibration of the image analyser was performed using a measuring tape attached to the inside of the wool section of the column as a reference.

**Table 1:** Photo capture parameters of the triple module camera.

Component	Characteristics
Main camera	64MP standard photos at 16MP (f1.8)
Secondary camera 1	2MP macro with fixed focus (f2.4)
Secondary camera 2	2MP depth sensor (f2.4)
Parameter	Value
White Balance (WB)	Automatic
Focus (F)	Full
Shutter priority (S)	1/30
Light sensitivity (ISO)	4000
Exposure value (EV)	0

**Db by CFD simulation**

The 35 experimental conditions established for the laboratory flotation column were simulated. During the simulation, the Cartesian coordinate system, Newtonian fluid, thermophysical properties were considered as constants due to no temperature changes, no friction on the walls containing the fluid, and the force of gravity acting vertically (on the Z axis). The dimensions of the venturi gas disperser and the flotation column remained constant during the simulations. To perform the CFD simulation, the model geometry was built in AutoCAD® and then exported to the ANSYS®

system. The model was developed in 3 dimensions, modelling the Venturi-type disperser and the flotation column with a diameter of 0.10m and a length of 2.6m.

Within the Meshing® sub application, the mesh was built to perform the finite volume analysis and subsequently in Fluent® the general parameters, internal models, characteristics of the materials to be used in the analysis, boundary conditions, solution methods and finally the model initialization were configured (Figure 2).

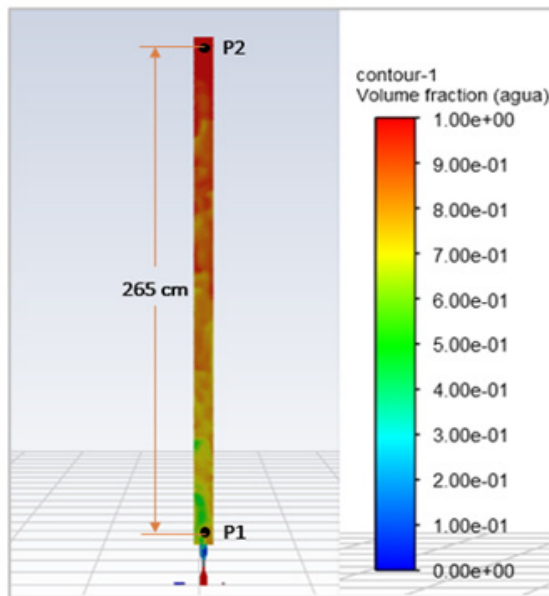


**Figure 2:** CFD simulation of 35 different flow conditions in the flotation column with the Venturi-type disperser.

**Result and Discussion**

Figures 3 & 4 are examples of photographic evidence obtained by this technique. Figure 3 corresponds to the case of water and air flows of 4L/min; the bubble diameters were traced manually. The results in general show that the number of bubbles generated

increases with the water and air flow rates, due to the increase in the pressure drop within the venturi; however, it can be seen in Figure 4 that the increase in the water and air flow rates (8L/min, and 10L/min, respectively), promotes bubble coalescence due to the generated turbulence.

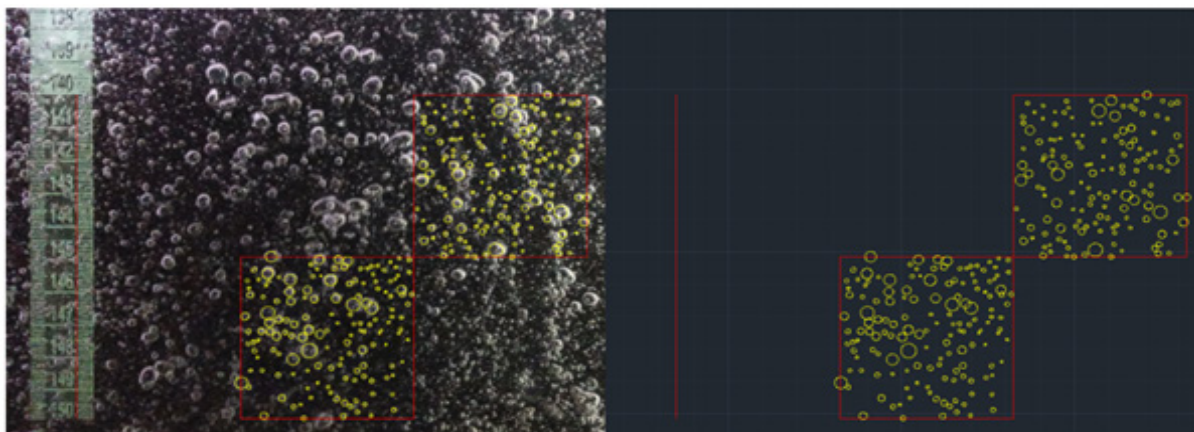


**Figure 3:** Photographs of bubbles produced with a liquid and gas flow rate of 4L/min.

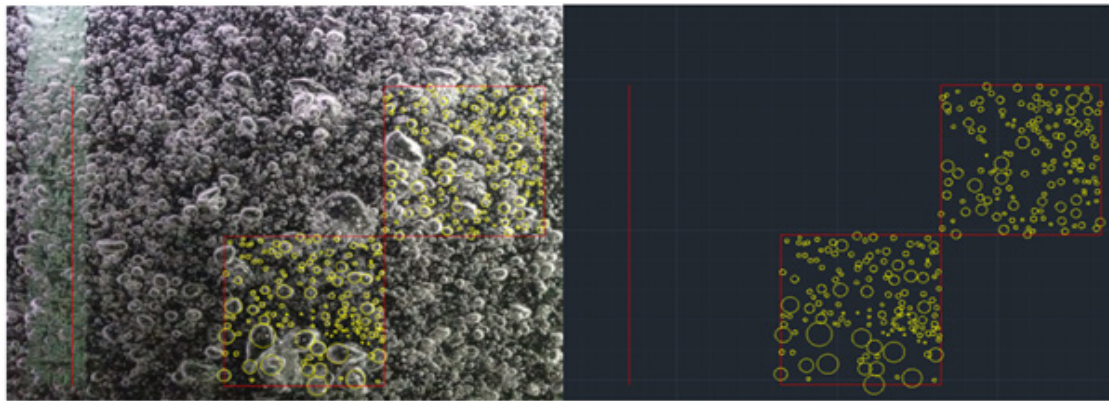


**Figure 4:** Bubbles produced with a water flow rate of 8L/min, and a gas flow rate of 10L/min.

From the above figures, it is evident that at lower flow rates a smaller quantity of bubbles is observed, but greater homogeneity in the diameters. In flotation systems, the goal is to generate the largest possible number of bubbles and with a relatively small size that results in high surface areas that allow the capture of the largest mass of valuable particles, and not to generate large bubbles that float or rise at high speed in the collection area, decreasing the probability of collision between bubbles and particles, which will ultimately decrease the efficiency of the flotation. On the other hand,

the wide distribution of  $D_b$  and the large number of them generate turbulence and coalescence due to the difference in the flotation speeds of the bubbles; this phenomenon decreases the surface area available to retain particles and the result will be a decrease in flotation efficiency. Table 2 shows the results of the estimation of bubble diameters by solving the Drift Flux equations, the diameters measured from photographic images and those predicted by CFD simulation, for all experimental conditions included in this work.

**Table 2:** Results of the  $D_{b80}$  by the photographic technique, the CFD simulation, and the Drift Flux model solution.

Liquid flow (Ql) L/min	Air flow (Qg), L/min	Db80, mm		
		Photographs	Predicted	Drift Flux
4	4	0.88	0.83	0.75
	5	1.45	1.54	1.22
	6	1.42	1.33	1.10
	7	1.45	1.62	1.24
	8	1.44	1.38	1.18
	9	1.43	1.60	1.19
	10	1.43	1.27	1.23
5	4	0.92	1.00	0.91
	5	0.88	0.78	0.87
	6	0.90	1.00	0.93
	7	0.98	0.91	1.01
	8	0.95	0.97	1.03
	9	1.42	1.29	1.36
	10	1.47	1.66	1.42
6	4	0.92	0.88	0.99
	5	0.96	1.04	1.17
	6	0.92	0.88	1.10
	7	1.47	1.59	1.60
	8	1.44	1.30	1.60
	9	1.44	1.50	1.33
	10	1.42	1.41	1.43
7	4	0.92	0.97	1.14

	5	1.47	1.31	1.70
	6	1.48	1.55	1.31
	7	1.46	1.39	1.37
	8	1.45	1.49	1.55
	9	1.42	1.38	1.25
	10	0.92	0.94	1.15
8	4	0.93	0.91	1.12
	5	0.94	1.03	1.12
	6	1.99	1.87	2.05
	7	1.46	1.61	1.79
	8	1.47	1.35	1.66
	9	1.44	1.56	1.56
	10	1.43	1.42	1.48

### Comparison of the diameters obtained

Figure 5 compares the Db80 bubble diameters derived from the three techniques included in this work, the one estimated by solving the equations of the Drift Flux model, the one measured as a result of the treatment of the photographs of the flat part of the column, and the one simulated by CFD; the above, using a Venturi bubble generator installed in the column used in the experiment.

From the figure above, the dashed line represents the +/- minus 20% divergence in the Db80 from the measured bubble diameter. It is observed that practically all bubble diameters fall within this 20%, which allows us to conclude that the Drift Flux estimation and CFD simulation prediction techniques reliably establish the Db80 generated by the venturi-type disperser in a flotation column for the air-water system.

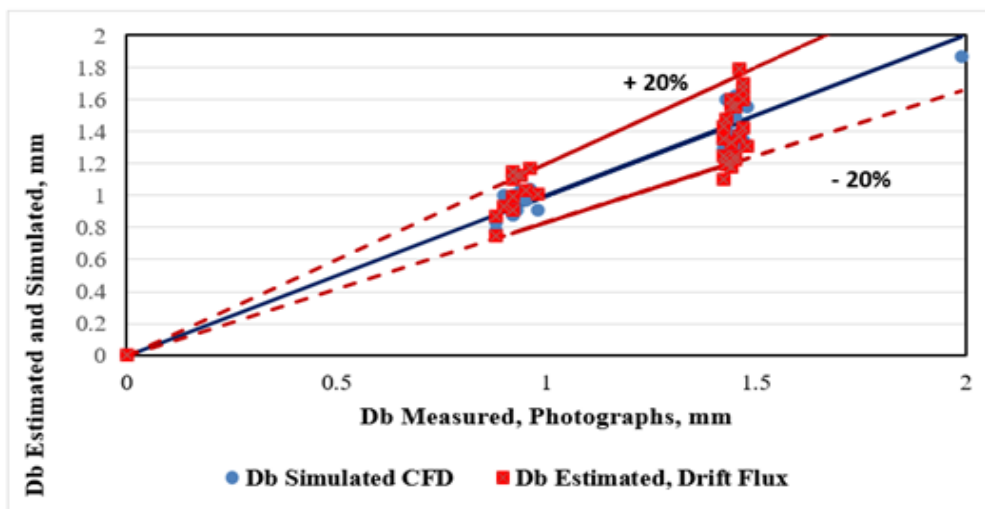


**Figure 5:** Comparison between estimated and measured Db80 in a laboratory flotation column. Dashed lines represent +/- 20 divergence from measured diameter.

### Conclusion

From the experimental work and CFD simulation of bubbles generated by a venturi-type disperser installed in a laboratory flotation column, for the air-water system, the following conclusions are derived: The Db80 simulated by CFD and estimated by solving the Drift Flux equations reasonably agree with the Db80 measured by acquiring dispersion photographs and corresponding image analysis. The simulated and estimated bubble diameters diverge by a maximum of 20% from the measured diameters. This will allow the simulation technique to be reliably applied to design gas

dispersion systems for air-water systems; for example, a venturi-type generator installed in a flotation column.

### Acknowledgement

The financial support for this work is from the UMSNH in Mexico. José Guadalupe González Valencia sincerely thanks CONAHCyT for the scholarship during his PhD studies through the grant (902631).

### References

- Gembe Huaroco JE, Escudero García R, Arcos Gutiérrez H (2018) CFD simulation of a sparger type venturi to generate bubbles in a two-phase flotation system. *Interciencia* 43(2): 263.

2. Arbiter N, Harris CC (1962) Flotation kinetics. AIME, New York, USA, pp. 215-246.
3. Diaz-Penafiel P, Dobby GS (1994) Kinetic studies in flotation columns: Bubble size effect. *Miner Eng* 7(4): 465-478.
4. Grau RA, Heiskanen K (2002) Visual technique for measuring bubble size in flotation machines. *Miner Eng* 15(7): 507-513.
5. Jameson GJ, Nam S, Moo-Young M (1977b) Physical factors affecting recovery rates in flotation. *Min Sci Eng* 9(3): 103-111.
6. Oscar RO (2023) Scientific photography. *Con-Ciencia scientific bulletin. Biannual Publication* 10(19): 44-46.
7. Cruz Gavilan Y, Hernández PV, Leyva AL, Gómez Águila MV, Chuairey CM (2020) Computational fluid dynamics: Review and analysis of applications in engineering. *Journal of Agricultural Technical Sciences* 29(4):
8. Finch JA, Dobby GS (1990) *Column Flotation*. Pergamon Press, Oxford, England.
9. Emerson B (2008) Bubble size control in flotation systems using variable-aperture jet gas dispersers. Undergraduate thesis. Institute of Metallurgical and Materials Research, UMSNH, Morelia, Mexico.
10. Grau RA, Laskowski JS (2006) Role of frothers in bubble generation and coalescence in mechanical flotation cell. *Can Chem Eng* 84(2): 170-182.
11. Kracht W, Vallebuona G (2005) Rate constant modelling for batch flotation, as a function of gas dispersion properties. *Minerals Engineering* 18(11): 1067-1076.
12. Tavera FJ, Escudero R, Finch JA (2001) Gas holdup in flotation columns: laboratory measurements. *International Journal of Mineral Processing* 61(1): 23-40.
13. Kulkarni AA, Joshi JB (2005) Bubble formation and bubble rise velocity in gas-liquid systems: A review. *Ind Eng Chem Res* 44(16): 5873-5931.
14. Mandal A, Kundu G, Mukherjee D (2005) A comparative study of gas holdup, bubble size distribution and interfacial area in a downflow bubble column. *Chemical Engineering Research and Design* 83(4): 423-428.
15. Silberman E (1960) Air-water mixture flow through orifices, bends, and other fittings in a horizontal pipe. Project Report No 63. St. Anthony Falls Hydraulic Lab. University of Minnesota, USA, pp. 253-494.
16. Michael S, Stefaan S, Stephen N, Jan C (2004) Effect of humic substances and particles on bubble coalescence and foam stability in relation to dissolved air flotation processes. *Physicochemical Problems of Mineral Processing* 38: 37-52.
17. Barigou M, Greaves M (1991) A capillary suction probe for bubble size measurement. *Meas Sci Technol* 2: 318-326.
18. Cheng YH, Mikhail MW, Salama AIA (1996) Bubble generation by a two-phase ejector. *Column 96, Third International Symposium on Column Flotation*.
19. Escudero R (2007) Mathematical models commonly used in dispersion systems to estimate their characteristics. SPUM Training and Development Program, UMSNH, Mexico.
20. Evans GM, Jameson GJ, Atkinson BW (1992) Prediction of the bubble size generated by a plunging liquid jet bubble column. *Chem Eng Science* 47(13-14): 3265-3272.